ORIGINAL ARTICLE

Combined impact of ROR2 and its ligands on the pathogenesis and prognosis of idiopathic pulmonary fibrosis

SEUNG-LEE PARK[1,*], JONG-UK LEE[2,*], MIN KYUNG KIM[1], EUNJEONG SEO[1], MYUNG-SHIN KIM[3], HUN GYU HWANG[2], JUNG HYUN KIM[4], HUN SOO CHANG[5], CHOON-SIK PARK[2]

[1]Department of Interdisciplinary Program in Biomedical Science Major, Soonchunhyang University, Asan, Republic of Korea; [2]Division of Allergy and Respiratory Medicine, Department of Internal Medicine, Soonchunhyang University Bucheon Hospital, Bucheon , Republic of Korea; [3]Division of Allergy and Respiratory Disease, Soonchunhyang University Gumi Hospital, Gumi, Republic of Korea; [4]Department of Internal Medicine, Soonchunhyang University Seoul Hospital, Seoul, Republic of Korea; [5]Department of Microbiology, College of Medicine, Soonchunhyang University, Cheonan, Republic of Korea.

*These authors contributed equally to this work

ABSTRACT

Background and aim: Idiopathic pulmonary fibrosis (IPF) is a progressive interstitial lung disease characterized by aberrant fibroblast activation and extracellular matrix accumulation. Although ROR2 signaling via Wnt ligands has been implicated in fibrosis, their integrated clinical relevance in IPF remains unclear. This study investigated the clinical significance of ROR2 and its ligands—WNT1, WNT5A, and WNT7A—in IPF development and prognosis.

Methods: Bronchoalveolar lavage (BAL) fluid was collected from 124 IPF patients and 17 controls. Protein levels of ROR2, WNT1, WNT5A, and WNT7A were measured using ELISA. Immunofluorescence staining was performed to evaluate cellular localization. Cox proportional hazards analysis with backward elimination was used to identify mortality risk factors. Kaplan–Meier and log-rank tests were used to compare cumulative mortality between subgroups.

Received: 11 September 2025 | Accepted: 27 December 2025

Correspondence: Choon-Sik Park, MD, Ph.D. / Division of Allergy and Respiratory Medicine, Department of Internal Medicine, Soonchunhyang University Bucheon Hospital, 170, Jomaru-ro, Wonmi-gu, Bucheon-si, Gyeonggi-do, 14584, Republic of Korea. /
Email: mdcspark@hanmail.net
Hun Soo Chang, Ph.D / Address: Department of Microbiology, College of Medicine, Soonchunhyang University, Cheonan 33151, Korea. Phone number: 82-32-621-5021, Fax: 82-32-621-5023 / Email: hschang@sch.ac.kr

Results: The levels of ROR2 and WNT7A were significantly higher in IPF compared to controls ($p < 0.001$ and $p = 0.030$, respectively). Among the proteins analyzed (ROR2, WNT1, WNT5A, and WNT7A), only elevated ROR2 levels were independently associated with increased mortality (hazard ratio [HR] = 2.32, $p = 0.026$), whereas WNT1, WNT5A, and WNT7A did not show significant associations with survival after correction for multiple comparisons using the Benjamini–Hochberg false discovery rate (FDR) method. Immunofluorescence analysis demonstrated co-localization of ROR2 with COL1A1-positive fibroblasts, as well as with WNT1, WNT5A, and WNT7A. Exploratory stratification based on combined ROR2 and WNT5A expression identified a subgroup with low ROR2 / high WNT5A levels that showed a trend toward better prognosis.

Conclusion: ROR2 levels in BAL fluid are independently associated with IPF pathogenesis and prognosis, and may serve as a useful biomarker for identifying molecular endotypes and assessing clinical risk. Exploratory findings suggest that ROR2 and its ligand may modulate prognosis in a subset of patients.

Key words: ROR2, idiopathic pulmonary fibrosis, WNT proteins, bronchoalveolar lavage fluid, mortality

Introduction

Idiopathic pulmonary fibrosis (IPF) is a chronic and progressive lung disease that often leads to death, and is marked by disordered lung tissue remodeling (1). At the cellular level, the condition involves the abnormal activation and proliferation of fibroblasts and myofibroblasts, which accumulate and deposit thick layers of extracellular matrix in the lung tissue (2-5). As the disease advances, these cells become excessively proliferative and develop resistance to apoptosis, contributing to the ongoing scarring of lung parenchyma (5, 6). These characteristic changes in fibroblast behavior ultimately disrupt normal alveolar structure and impair respiratory function. However, the molecular mechanisms that continue to drive this destructive "fibrotic loop" are still not fully understood and remain an active subject of scientific research. Recent studies have increasingly pointed to a role for Wingless-type MMTV integration site (Wnt) signaling in the disrupted tissue repair processes seen in IPF (7-10). WNT proteins play essential roles in regulating cell fate decisions, proliferation, and regeneration, and abnormal activation of the Wnt/β-catenin pathway has been documented in fibrotic lungs (7, 8). In fact, canonical Wnt signaling is upregulated in IPF, and blocking this pathway experimentally has been shown to reduce fibrotic progression (10). Several Wnt ligands and downstream targets are misregulated in IPF; for instance, WNT1-inducible signaling protein-1 (WISP1), which is a direct target of WNT1, is overexpressed in alveolar epithelial cells in fibrotic lung tissue (11). The noncanonical WNT5A ligand is also found at elevated levels in IPF and has been shown to promote fibroblast proliferation and survival while suppressing apoptosis (12). More recently, basal-like epithelial cells within fibrotic regions of the lung have been found to release high amounts of WNT7A, which can activate nearby fibroblasts (13). Taken together, this evidence indicates that both canonical (such as WNT1/WISP1) and noncanonical (such as WNT5A and WNT7A) Wnt pathways may contribute to sustained fibroblast activation and ongoing extracellular matrix production in IPF. Receptor tyrosine kinase-like orphan receptor 2 (ROR2) has recently gained attention as a key Wnt co-receptor in the context of pulmonary fibrosis. ROR2 is a transmembrane protein that contains cysteine-rich domains capable of binding Wnt ligands, and it mainly serves as a receptor for WNT5A, playing a central role in mediating noncanonical Wnt signaling (14). Significantly, ROR2 expression is highly elevated in IPF. In fibroblasts isolated from IPF patients, ROR2 mRNA levels are reported to be over 20 times higher than those in controls (15). The interaction between ROR2

and WNT5A has functional implications, including modulation of downstream Wnt/β-catenin activity and enhanced fibroblast accumulation via resistance to apoptosis (12, 16). Clinically, ROR2 protein is found at much higher levels in the bronchoalveolar lavage (BAL) fluid of IPF patients compared to controls or those with other interstitial lung diseases (16), and its concentration has been associated with more severe stages of the disease (16). These findings suggest that the ROR2–Wnt signaling axis is not only biologically significant in fibroblast dysregulation but may also have clinical utility as both a biomarker and therapeutic target in IPF (16). Nonetheless, the broader clinical significance of ROR2 and its ligands—WNT1, WNT5A, and WNT7A—has yet to be fully explored. In the present study, we sought to clarify this by measuring the levels of ROR2 and WNT proteins in BAL fluid from patients with IPF and matched controls, and by analyzing their spatial distribution in lung tissue samples from individuals with IPF.

Methods

Study subjects

BAL fluids were obtained from the biobank of Soonchunhyang University Hospital, Bucheon, Korea, following approval by the Institutional Ethics Committee (Approval No. SCHBC 2022-08-020-001). Informed consent was obtained from all participants prior to sample collection. All participants underwent comprehensive clinical evaluation, including chest radiography, high-resolution computed tomography (HRCT), and pulmonary function testing, specifically forced vital capacity (FVC) and diffusion capacity for carbon monoxide (DL_{CO}). BAL procedures were performed within two weeks of the initial evaluation, during which patients remained clinically stable without signs of infection or acute exacerbation. IPF was diagnosed either by histopathologic confirmation of a usual interstitial pneumonia pattern (n = 64), or through multidisciplinary discussion in accordance with the 2011 and 2018 international diagnostic guidelines (n = 60) (17, 18). Controls were asymptomatic, as verified using a standardized respiratory symptom questionnaire, and showed normal pulmonary function (predicted FEV1 and FVC > 80%) along with unremarkable chest radiographs.

Enzyme-linked immunosorbent assay (ELISA) of ROR2 and Wnt ligands in BAL fluid

BAL was performed within 2 weeks of the initial examination in a stable condition without signs of infection or acute exacerbation. In patients with IPF, BAL was obtained from the most significantly involved lower lobe segments as determined by HRCT, whereas in controls it was obtained from the right middle lobe (19-21). The mean BAL fluid recovery rate was 42.3% in IPF and 52.7% in controls, consistently exceeding the recommended 30% threshold, ensuring sample quality. All BAL samples were processed and stored under identical standardized conditions. None of the patients were receiving immunosuppressive treatment at the time of BAL collection. Total cell counts were determined using a hemocytometer. BAL fluid was centrifuged at 500 × g for 5 minutes to separate cellular components, which were then utilized for cytological examination. The remaining acellular BAL fluid, not required for clinical diagnostics, was aliquoted and stored at −80°C in the institutional biobank. Differential cell counts were performed on 500 cells per sample using cytocentrifuge-prepared slides stained with Diff-Quick. Protein concentrations of ROR2, WNT1, WNT5A, and WNT7A in BAL fluid were quantified using commercially available ELISA kits: ROR2 (MBS9326623, MyBioSource, CA, USA), WNT1 (BSKH66231, Bioss, MA, USA), WNT5A (BSKH66237, Bioss, USA), and WNT7A (BSKH66239, Bioss, USA), according to manufacturers' instructions. The lower limits of detection were 0.05 ng/mL for ROR2, 0.01 ng/mL for WNT1, 0.07 ng/mL for WNT5A, and 5.2 pg/mL for WNT7A.

Immunofluorescence (IF) staining of ROR2 and WNT proteins in lung tissue

Formalin-fixed, paraffin-embedded lung tissue samples were collected from patients with IPF and controls who underwent lobectomy for stage I or II lung cancer. Control lung tissues were confirmed to

be free of malignant cells by hematoxylin and eosin (H&E) staining. Tissue sections were cut at a thickness of 4 μm, followed by deparaffinization and rehydration, and subsequently post-fixed in 0.4% cold paraformaldehyde for 30 minutes at room temperature. To prevent nonspecific binding, slides were incubated for 1 hour with Fc receptor blocking reagent (Innovex Biosciences, Richmond, CA, USA) containing 5% bovine serum albumin. Sections were then incubated overnight at 4°C with the following primary antibodies: rabbit polyclonal anti-human ROR2 (1:50; Invitrogen, Waltham, MA, USA), mouse monoclonal anti-human COL1A1 (1:400; Bioss, Woburn, MA, USA), mouse monoclonal anti-human WNT1 (1:100; Santa Cruz Biotechnology, Dallas, TX, USA), mouse monoclonal anti-human WNT5A (1:100; Santa Cruz), and mouse monoclonal anti-human WNT7A (1:100; Santa Cruz). After three washes with Tris-buffered saline, sections were incubated for 1 hour at room temperature with species-specific secondary antibodies: anti-rabbit IgG H&L (FITC) (1:500; Abcam, Cambridge, UK) and anti-mouse IgG H&L (Alexa Fluor™ 594) (1:500; Invitrogen, Waltham, MA, USA). Nuclei were counterstained using a 4′,6-diamidino-2-phenylindole (DAPI)-containing mounting medium (ab104139; Abcam). Fluorescence images were acquired using a confocal laser scanning microscope (LSM 510 META; Zeiss, Jena, Germany) equipped with a CoolSNAP HQ camera (Photometrics, Tucson, AZ, USA). Image processing was performed using ZEN 2009 Light Edition software (Zeiss). After uniform background subtraction, regions of interest (ROIs) were manually selected to minimize background interference. Manders' coefficients M1 and M2, ranging from 0 (no colocalization) to 1 (complete colocalization), were calculated to quantify fluorescence overlap using the Coloc2 plugin in Fiji (ImageJ, NIH), following the methodology described by Shakhov et al. (2022) (22). Six images were analyzed per group.

Statistical analysis

All statistical analyses were performed using SPSS version 22.0 (IBM Corp., Armonk, NY, USA). Data normality was assessed using the Shapiro–Wilk test. Variables with non-normal distributions are presented as medians with interquartile ranges (25th–75th percentiles). Continuous variables are presented as mean ± standard error of the mean or median (interquartile range), as appropriate. Comparisons between two groups were performed using the Mann–Whitney U test for non-normally distributed variables. Comparisons among three or more groups were performed using the Kruskal–Wallis test for non-normally distributed variables or one-way analysis of variance (ANOVA) for normally distributed variables, followed by Bonferroni post hoc correction. Categorical variables were compared using the chi-square test or Fisher's exact test, as appropriate. A p-value < 0.05 was considered statistically significant. Receiver operating characteristic (ROC) curve analysis was used to evaluate the diagnostic performance of biomarkers. Optimal cut-off values were determined using the Youden index. Comparisons between areas under the ROC curves (AUC) were performed using the Z-test, following the method described by DeLong et al. (23). Kaplan–Meier survival curves were constructed to compare cumulative mortality between groups, and multivariate analysis of mortality was performed using Cox proportional hazards regression. To correct for multiple comparisons in the Cox analyses, the Benjamini–Hochberg false discovery rate (FDR) method was applied where appropriate. Age and sex were retained in all models as clinically relevant covariates, whereas smoking history, FVC, DL_{CO}, and each biomarker were included if their univariate association reached $p < 0.1$. The proportional hazards assumption was verified using Schoenfeld residuals. The event-per-variable ratio was approximately 8.3, which is considered acceptable for exploratory survival analyses. A p-value < 0.05 was considered statistically significant.

Results

Clinical characteristics of the study groups

BAL samples were collected from 124 patients with IPF and 17 controls (Table 1). Compared to controls, patients with IPF exhibited significantly elevated total BAL cell counts, along with increased proportions of neutrophils, eosinophils, and lymphocytes

Table 1. Comparison of clinical characteristics of the study subjects who underwent BAL.

Variables	Controls	IPF	p-value
No.	17	124	-
Age (year)	52 (44-62)	65.5 (59.75-73)	< 0.001
Sex (male/female)	11/6	84/40	0.044
Smoke (SM/ES/NS)	4/4/9	23/41/60	< 0.001
Survival/Death	ND	74/50	-
Follow up duration (years)	ND	4.67 (1.65-7.31)	-
FVC (% pred.)	87.8 ± 10.7	73.2 ± 16.9	< 0.001
DL_{CO} (% pred.)	91 ± 18.5	69.2 ± 20.9	< 0.001
Treatment status			
Anti-fibrotic agent (%)	-	28 (22.6)	
Anti-inflammatory agents (%)	-	113 (91.1)	
BAL fluid recovery rate (%)	51.5 ± 2.8	40.7 ± 5.2	-
BAL total cell count ($\times 10^5$/mL)	1.71±0.7	6.33±1.82	< 0.001
Macrophages (%)	94.3 ± 4.2	67.5 ± 24.7	< 0.001
Neutrophils (%)	2.6 ± 2.6	24.6 ± 25.4	< 0.001
Eosinophils (%)	0.4 ± 0.9	2.9 ± 3.5	< 0.001
Lymphocytes (%)	2.7 ± 2.5	5.1 ± 5.4	< 0.001

Abbreviations: IPF: Idiopathic pulmonary fibrosis, SM/ES/NS: smokers/ex-smokers/never-smokers, FVC: forced vital capacity, DL_{CO}: diffusing capacity of the lung for carbon monoxide, BAL: bronchoalveolar lavage. Data with skewed distributions are presented as median (25th–75th quartiles), and comparisons between two groups were performed using the Mann–Whitney U-test. Data with normal distributions are presented as mean ± standard error of the mean.

($p < 0.001$, respectively). Pulmonary function testing revealed significantly reduced FVC ($p < 0.001$) and DL_{CO} ($p < 0.001$) in the IPF group compared to controls.

Comparison of ROR2 and Wnt protein levels in BAL fluid between groups

ROR2 protein was detected in 109 of 124 patients with IPF (87.9%) and in 1 of 17 controls (5.9%). WNT1 was detected in 100 of 124 IPF patients (80.6%) and 15 of 17 controls (88.2%), WNT5A in 89 of 124 IPF patients (71.8%) and 9 of 17 controls (52.9%), and WNT7A in 82 of 124 IPF patients (66.1%) and 8 of 17 controls (47.1%). Chi-square analysis revealed that the detection rate of ROR2 was significantly higher in IPF patients compared to controls ($p < 0.001$), whereas no statistically significant differences were observed in the detection rates of WNT1, WNT5A, or WNT7A between the groups (Table S1).

Patients with IPF showed significantly elevated levels of ROR2 and WNT7A in BAL fluid compared to controls ([1.86 (0.39–5.55) ng/mL vs. 0 ng/mL, $p < 0.001$]; [8.73 (0–22.35) ng/mL vs. 5.78 (0–7.01) ng/mL, $p = 0.030$], respectively). Although WNT1 and WNT5A levels tended to be higher in the IPF group, these differences did not reach statistical significance ([0.11 (0.03–0.23) ng/mL vs. 0.06 (0.02–0.16) ng/mL, $p = 0.484$]; [9.00 (0–21.00) ng/mL vs. 1.00 (0–10.00) ng/mL, $p = 0.118$], respectively) (Figure 1).

ROC curve analysis demonstrated that ROR2 exhibited strong discriminative capacity between IPF and controls in the unadjusted analysis, whereas WNT1, WNT5A, and WNT7A showed limited diagnostic performance (Figure 2A). After age adjustment, all four biomarkers retained or improved their discriminative ability (Figure 2B). Detailed metrics, including AUC, cut-off values, sensitivity, specificity, and p-values, are summarized in Figure 2C.

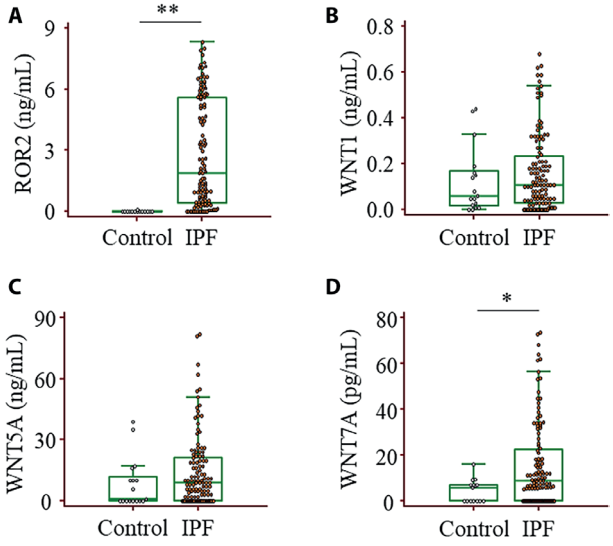

Figure 1. ROR2 and Wnt protein concentrations in BAL fluids. (A-D) ROR2, WNT1, WNT5A, and WNT7A protein levels were measured by ELISA in BAL fluids from patients with IPF (n = 124) and controls (n = 17). Values below the manufacturer's lower limit of detection (LOD) were assigned a value of 0 ng/mL (or pg/mL) for statistical analysis, as they were below the quantifiable range. The LODs were 0.05 ng/mL for ROR2, 0.01 ng/mL for WNT1, 0.07 ng/mL for WNT5A, and 5.2 pg/mL for WNT7A. Detection rates were as follows: ROR2, 109/124 (87.9%) in IPF and 1/17 (5.9%) in controls; WNT1, 100/124 (80.6%) in IPF and 15/17 (88.2%) in controls; WNT5A, 89/124 (71.8%) in IPF and 9/17 (52.9%) in controls; WNT7A, 82/124 (66.1%) in IPF and 8/17 (47.1%) in controls. Data are presented as medians with interquartile ranges (25th and 75th percentiles). Statistical differences were assessed using the Mann–Whitney U test. $^{*}p < 0.05$, $^{**}p < 0.01$.

Comparison of mortality rates in patients with IPF based on ROR2 and Wnt levels

In the ROC analysis, the AUC values were used as C-indices to determine optimal cut-off levels for survival stratification using Youden's index. Although the p-values for WNT1 and WNT7A were not significant, their cut-off values were used to define high- and low-expression groups for exploratory survival comparison. Among these, ROR2 demonstrated statistically significant discrimination, whereas WNT5A showed an initial association with survival that did not remain significant after adjustment for multiple comparisons using the FDR method. WNT1 and WNT7A exhibited non-significant but biologically plausible trends. The optimal cut-off values determined by Youden's index were 5.59 ng/mL for ROR2 (AUC = 0.653, p = 0.022), 0.01 ng/mL for WNT1 (AUC = 0.521, p = 0.711), 6 ng/mL for WNT5A (AUC = 0.594, p = 0.041), and 20.97 pg/mL for WNT7A (AUC = 0.524, p = 0.673). Cumulative mortality analysis revealed that patients with ROR2 levels ≥ 5.59 ng/mL exhibited significantly higher mortality compared to those with ROR2 < 5.59 ng/mL (hazard ratio [HR] = 2.32; 95% confidence interval [CI]: 1.29–4.18; p = 0.003) (Figure 3A). Patients with WNT1 levels ≥ 0.01 ng/mL showed higher mortality rates than those with lower levels, although this difference did not reach statistical significance (HR = 2.49; 95% CI: 0.89–6.99; p = 0.071) (Figure 3B). For WNT5A, patients with levels ≥ 6 ng/mL demonstrated lower mortality compared with those with lower levels (HR = 0.52; 95% CI: 0.29–0.94; p = 0.028) (Figure 3C). However, this association did not reach statistical significance after correction for multiple comparisons using FDR method (adjusted p = 0.056; Table 2). For WNT7A, patients with levels ≥ 20.97 pg/mL exhibited a non-significant trend toward reduced mortality (HR = 0.72; 95% CI: 0.35–1.50; p = 0.377) (Figure 3D).

Univariate analysis identified FVC (p = 0.008), DL_{CO} (p = 0.013), ROR2 (p = 0.005), and WNT5A (p = 0.031) as predictors of mortality. However, the association of WNT5A did not remain statistically significant after adjustment for multiple comparisons using the FDR method (adjusted p = 0.056). In the multivariate Cox regression analysis with backward selection, only FVC (p = 0.002) and ROR2 (p = 0.024) remained independently associated with mortality (Table 2).

Correlation of clinical parameters with combined ROR2 and WNT5A expression in BAL fluid

ROR2 and its ligand WNT5A were selected for analysis due to their relevance to non-canonical Wnt signaling in IPF. WNT5A was significant in the initial Cox regression but lost significance after FDR adjustment; accordingly, its cutoff was applied on an exploratory basis. Patients with IPF were then stratified into four groups according to BAL fluid levels of ROR2 and WNT5A. The groups were defined as Group A

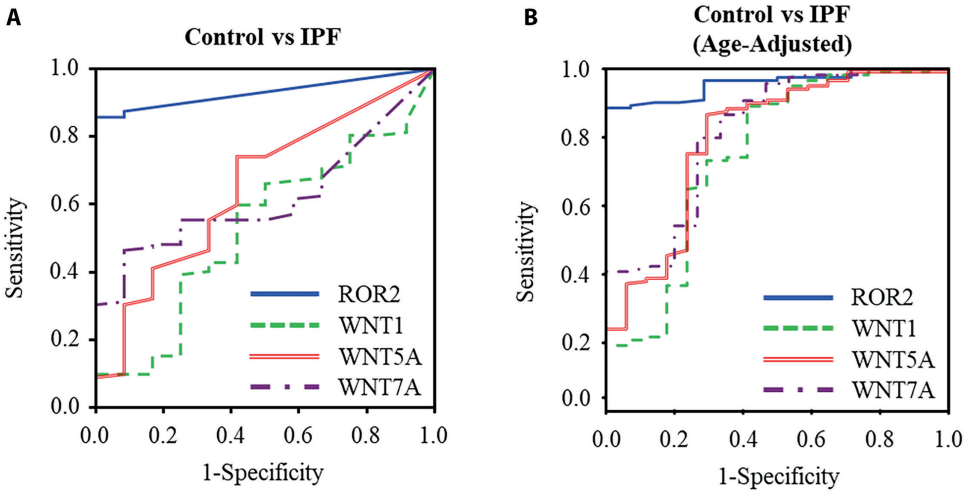

C

	Unadjusted					
	AUC	cut-off	95% CI	Sensitivity	Specificity	*p*-value
ROR2	0.931	0.06 ng/mL	0.886 – 0.976	85.7	100	< 0.001
WNT1	0.530	0.08 ng/mL	0.362 – 0.698	59.8	58.3	0.735 (NS)
WNT5A	0.652	1.50 ng/mL	0.492 – 0.812	74.1	58.3	0.085 (NS)
WNT7A	0.622	9.59 pg/mL	0.499 – 0.744	46.4	91.7	0.167 (NS)
	Age-Adjusted					
	AUC	Probability	95% CI	Sensitivity	Specificity	*p*-value
ROR2	0.959	0.82	0.926 – 0.991	88.6	100	< 0.001
WNT1	0.751	0.79	0.601 – 0.901	89.2	58.8	< 0.001
WNT5A	0.800	0.81	0.673 – 0.928	86.8	70.6	< 0.001
WNT7A	0.818	0.81	0.693 – 0.943	86.7	66.7	< 0.001

Figure 2. ROC curve analysis for the diagnosis of IPF versus controls. (A) Unadjusted ROC curves for ROR2, WNT1, WNT5A, and WNT7A based on single biomarker measurements. (B) Age-adjusted ROC curves from logistic regression models including age. Cut-off values represent predicted probabilities. (C) Summary of AUC, cut-off, 95% CI, sensitivity, specificity, and p-values. For age-adjusted analyses, cut-off values represent predicted probabilities. Abbreviations: AUC: area under the curve; CI: confidence interval; p-values ≥ 0.05 are marked as "(NS)" to indicate non-significance.

(ROR2↓/WNT5A↓, n = 36), Group B (ROR2↓/WNT5A↑, n = 54), Group C (ROR2↑/WNT5A↓, n = 12), and Group D (ROR2↑/WNT5A↑, n = 18) (Table 3).

Significant intergroup differences were observed in mortality rates, total BAL total cell counts ($\times 10^5$/mL), and neutrophils (%) ($p < 0.05$, respectively). Among the groups, Group B had the lowest mortality risk. HR were estimated using univariate Cox proportional hazards regression models. Specifically, Group A exhibited a significantly higher mortality risk compared to Group B (HR = 2.67; 95% CI: 1.22–5.84; p = 0.014). Additionally, Group B showed significantly lower mortality risks than Group C (HR = 0.27; 95% CI: 0.11–0.71; p = 0.008) and Group D (HR = 0.29; 95% CI: 0.13–0.67; p = 0.004). No significant differences in mortality risk were found among Groups A, C, and D (Figure 4).

Localization of ROR2 and WNT proteins in IPF lung tissue

To identify the cellular source of ROR2 expression in IPF lungs, IF double staining was performed using antibodies against ROR2 and COL1A1, a fibroblast marker (Figure 5A). The analysis demonstrated

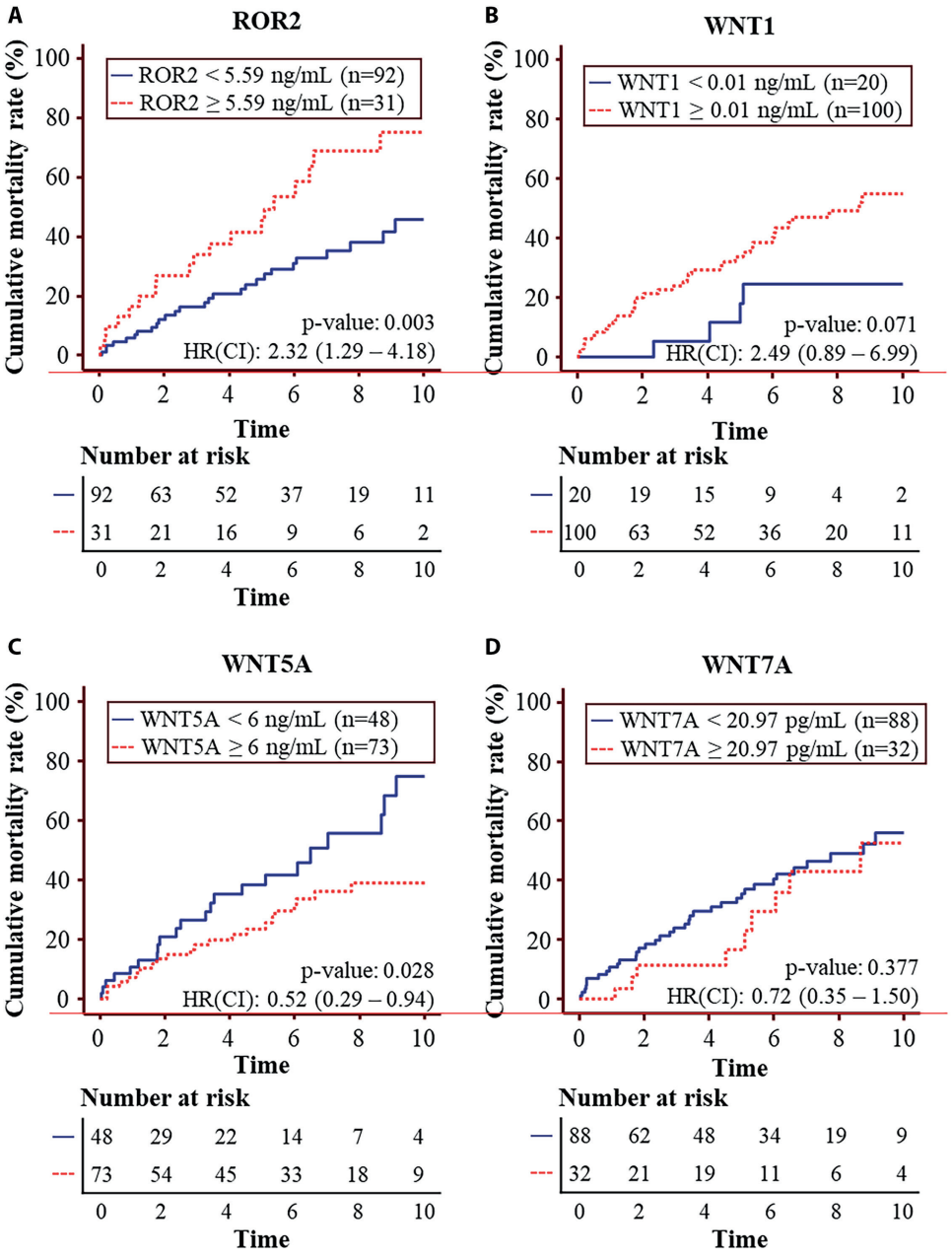

Figure 3. Exploratory comparison of 10-year mortality according to data-derived thresholds of ROR2 and WNT concentrations in BAL fluid from patients with IPF. (A) Mortality comparison based on the exploratory ROR2 threshold (5.59 ng/mL). (B) Mortality comparison based on the exploratory WNT1 threshold (0.01 ng/mL). (C) Mortality comparison based on the exploratory WNT5A threshold (6 ng/mL). (D) Mortality comparison based on the exploratory WNT7A threshold (20.97 pg/mL). Thresholds represent exploratory, data-derived values, not validated clinical cut-offs. Mortality rates were compared between groups above and below each threshold. Number at risk below the cumulative mortality curves represents the number of patients who remained under observation without experiencing the event (death) at each time point. P-values shown on the plots correspond to comparisons between groups, and hazard ratios (HR) with 95% confidence intervals (CI) are from Cox regression analyses presented in Table 2.

Table 2. Univariate and multivariate Cox regression analyses of clinical parameters and ROR2 and Wnt protein concentrations in BAL fluids for mortality.

Univariate analysis			
Parameters	**HR (95% CI)**	**p-value**	**FDR**
Age	1.03 (1.00 – 1.06)	0.076	0.137
Sex	1.00 (0.54 – 1.85)	0.994	0.994
Smoke	0.90 (0.62 – 1.31)	0.575	0.639
FVC (% pred.)	0.97 (0.96 – 0.99)	0.008	0.026
DL_{CO} (% pred.)	0.98 (0.97 – 1.00)	0.013	0.043
BAL fluids			
ROR2 (≥ 5.59 ng/mL)	2.32 (1.29 – 4.18)	0.005	0.026
WNT1 (≥ 0.01 ng/ml)	2.48 (1.18 – 5.22)	0.071	0.137
WNT5A (≥ 6 ng/mL)	0.52 (0.28 – 0.97)	0.031	0.056
WNT7A (≥ 20.97 pg/mL)	0.72 (0.36 – 1.40)	0.377	0.475
Multivariate analysis			
Parameters	**HR (95% CI)**	**p-value**	**FDR**
FVC (% pred.)	0.97 (0.94 – 0.99)	0.002	0.002
ROR2 (≥ 5.59 ng/mL)	2.33 (1.12 – 4.85)	0.024	0.024

Variables that showed a p-value < 0.05 in univariate analysis were included in the multivariate Cox regression model using a backward stepwise selection method. Hazard ratio (HR) and 95% confidence interval (CI) are presented. P-values were adjusted for multiple comparisons in the univariate analyses using the FDR method, where appropriate. Abbreviations: FVC: forced vital capacity, DL_{CO}: diffusing capacity for carbon monoxide, BAL: bronchoalveolar lavage.

Table 3. Comparison of clinical parameters among four IPF patient groups classified by BAL fluid ROR2 and WNT5A levels based on cut-off values.

Parameters	**Group A (ROR2↓ / WNT5A↓)**	**Group B (ROR2↓ / WNT5A↑)**	**Group C (ROR2↑ / WNT5A↓)**	**Group D (ROR2↑ / WNT5A↑)**	**p-value**
No.	36	54	12	18	-
Age (year)	67 (62.75 - 70.5)	63 (58.25 - 69)	68 (60.25 - 73)	74.5 (62.25 - 77.75)	0.055
Sex (male/female)	25 / 11	35 / 19	10 / 2	12 / 6	0.662
Smoke (CS/ES/NS)	7 / 14 / 13	8 / 15 / 24	4 / 5 / 2	3 / 6 / 9	0.185
Survival/Death	21 / 15	43 / 11*	5 / 7†	7 / 11†	0.002
Follow up duration (year)	3.26 (1.4 - 6.33)	5.94 (1.94 - 8.31)	4.31 (0.77 - 6.05)	3.79 (2 - 6.48)	0.163
FVC (% pred.)	69.5 (63.5 - 84.25)	75.5 (62.25 - 85)	74 (59.75 - 79.25)	78 (67.5 - 80)	0.838
DL_{CO} (% pred.)	68 (59.5 - 80)	70 (56.5 - 85)	62.5 (52.5 - 70.75)	64 (55 - 78.25)	0.745
BAL fluids					
ROR2 (ng/mL)	0.27 (0 - 1.11)	1.46 (0.53 - 3.27)*	6.19 (5.9 - 7.09)*†	6.54 (5.98 - 6.99)*†	< 0.001
WNT5A (ng/mL)	0 (0 - 2)	19 (10.25 - 27.5)*	0 (0 - 3)†	16.5 (9 - 21.5)*§	< 0.001
BAL total cell count (×105/mL)	3.08±6.83	5.55±7.09*	0.93±1.14†	4.19±5.48*§	0.005
Macrophages (%)	61.35 ± 26.21	62.45 ± 26.78	48.33 ± 22.61	51.29 ± 28.7	0.137

Table 3 (*Continued*)

Parameters	Group A (ROR2↓ / WNT5A↓)	Group B (ROR2↓ / WNT5A↑)	Group C (ROR2↑ / WNT5A↓)	Group D (ROR2↑ / WNT5A↑)	p-value
Neutrophils (%)	16.12 ± 19.91	20.95 ± 21.72	41.96 ± 22.76*†	35.21 ± 25.96*†	< 0.001
Eosinophils (%)	1.96 ± 2.61	2.68 ± 4.35	1.48 ± 0.71	3.62 ± 7.9	0.877
Lymphocytes (%)	6.54 ± 6.61	3.8 ± 3.24	2.65 ± 3.18	3.21 ± 2.93	0.179

Abbreviations: SM/ES/NS: smokers/ex-smokers/ never-smokers FVC: forced vital capacity, DL_{CO}: diffusing capacity of the lung for carbon monoxide, BAL: bronchoalveolar lavage. Data with skewed distributions are presented as median (25th–75th quartiles). Comparisons among four groups (A–D) were performed using the Kruskal–Wallis test, followed by Mann–Whitney U-tests with Bonferroni correction for post-hoc pairwise comparisons. Data with normal distributions are presented as mean ± standard error of the mean. Comparisons among four groups were performed using one-way analysis of variance (ANOVA), followed by Bonferroni post-hoc correction. * P < 0.05 compared to group A, † P < 0.05 compared to group B and § P < 0.05 compared to group C.

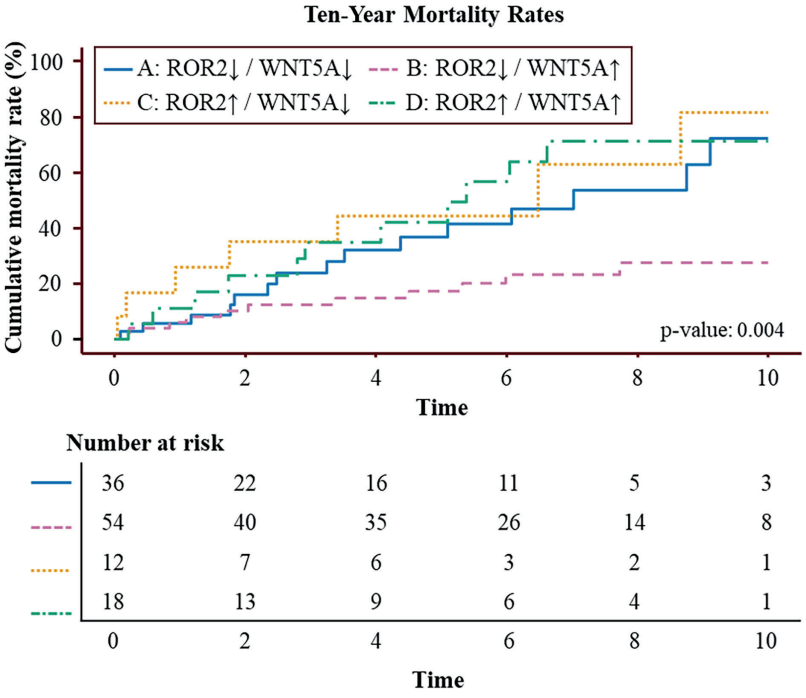

Groups	HR (95% CI)	*p*-value
A vs B	2.67 (1.22 – 5.58)	0.014
A vs C	0.68 (0.28 – 1.68)	0.405
A vs D	0.76 (0.35 – 1.65)	0.481
B vs C	0.27 (0.11 – 0.71)	0.007
B vs D	0.29 (0.13 – 0.67)	0.003
C vs D	1.07 (0.41 – 2.76)	0.891

Figure 4. Exploratory comparison of 10-year mortality based on combined data-derived thresholds of ROR2 and WNT5A concentrations in BAL fluid. Patients were categorized into four groups according to whether their ROR2 (5.59 ng/mL) and WNT5A (6 ng/mL) concentrations were above or below exploratory, data-derived thresholds. Cumulative mortality curves were used to explore differences in 10-year mortality across the four groups. Numbers at risk shown below the curves represent patients who remained under observation without experiencing the event (death) at each time point. Hazard ratios (HR) with 95% confidence intervals (CI) and corresponding p-values were obtained using unadjusted Cox proportional hazards regression analysis, applying the same exploratory thresholds used for group stratification. These thresholds are preliminary and not intended as validated clinical cut-off values.

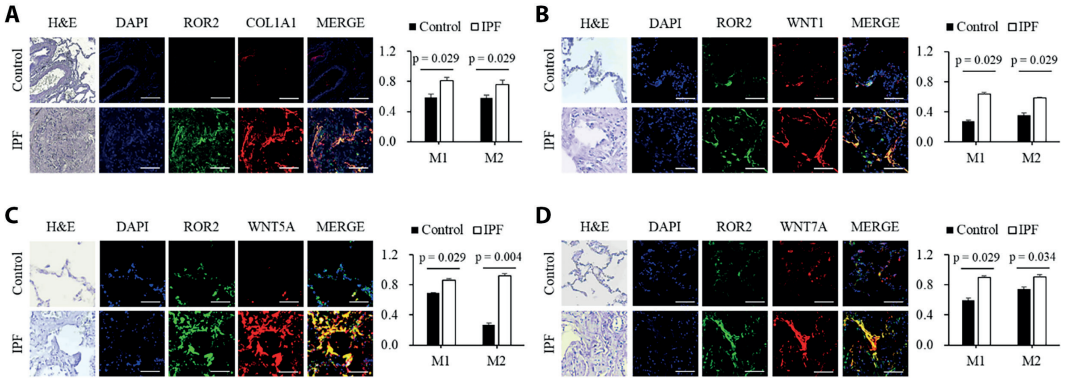

Figure 5. IF Staining of ROR2 with COL1A1 and WNT proteins in human lung tissues. (A–D) Representative images showing the expression of COL1A1 and WNT proteins, co-localized with ROR2 in human lung tissues. Quantitative analyses of Manders' coefficients (M1 and M2) were performed using the Coloc2 plugin in Fiji (ImageJ), demonstrating increased spatial co-localization between ROR2 and COL1A1/WNT proteins in IPF lungs compared with controls. Images were acquired at ×400 magnification. Scale bar = 200 μm.

clear co-localization of ROR2 with COL1A1, indicating that ROR2 is predominantly expressed in fibroblasts within fibrotic lung tissue. To investigate potential interactions within the ROR2–Wnt pathway, additional IF double staining was conducted for ROR2 together with the Wnt ligands WNT1, WNT5A, and WNT7A. ROR2 showed spatial co-localization with all three ligands in IPF lung samples, suggesting that these molecules may coexist within the same fibrotic niche rather than demonstrating direct regulatory relationships. Expression levels of ROR2, WNT1, WNT5A, and WNT7A were higher in IPF lung tissues compared with controls, as illustrated in Figures 5B–D. These findings support the presence of a ROR2–Wnt signaling milieu in the fibrotic microenvironment of IPF lungs, although the functional implications require further investigation.

Discussion

This study provides novel insights into the biological and clinical significance of ROR2 and its associated WNT ligands—WNT1, WNT5A, and WNT7A—in IPF. Our findings suggest that the ROR2–WNT signaling milieu is active within the fibrotic lung microenvironment and may influence fibroblast behavior. We observed significantly elevated levels of ROR2 and WNT7A in the BAL fluid of patients with IPF, consistent with prior studies (16). IF analysis demonstrated clear co-localization of ROR2 with the fibroblast marker COL1A1, confirming its enrichment in (myo)fibroblasts within fibrotic lesions. ROR2 was also spatially co-localized with WNT1, WNT5A, and WNT7A in situ, indicating that these molecules reside within the same fibrotic niche, although the directionality and functional relevance of these interactions remain to be clarified. In our survival analyses, elevated BAL fluid ROR2 levels were significantly associated with increased mortality, supporting its potential as a prognostic biomarker. In contrast, higher WNT5A levels were associated with improved survival in univariate analysis, but this relationship did not remain statistically significant after Bonferroni correction; therefore, interpretations involving WNT5A must be made cautiously. Although our findings do not establish a significant prognostic role for WNT5A in BAL fluid, previous studies indicate that WNT5A can exert divergent effects depending on receptor context and cellular origin, acting as a pro-fibrotic factor in some settings while counteracting canonical Wnt/β-catenin pathways in others (12, 24-26). The WNT5A detected in BAL fluid may originate from epithelial or immune cells and could reflect a compensatory or injury-responsive signal rather than direct fibroblast activation (27). Further research is needed to elucidate its biological role in IPF and determine whether it represents a context-dependent modulator or a marker of

disease adaptation. WNT5A alone was not independently associated with survival after Bonferroni correction. However, when analyzed in combination with ROR2, the subgroup analysis identified a subset of patients with low ROR2 and high WNT5A levels who exhibited lower mortality rates and reduced inflammatory cell counts. This indicates that the combined analysis revealed patterns not apparent from WNT5A alone and may reflect underlying heterogeneity in IPF or interactions within the ROR2–WNT signaling pathway. Because WNT5A was not independently significant, these findings should be considered exploratory. Nevertheless, they suggest the possibility of a distinct IPF endotype associated with ROR2–WNT signaling, although its clinical implications remain preliminary and require further validation. Beyond IPF, ROR2 has been implicated in a range of diseases, including cancer, osteoarthritis, and cardiovascular disorders. In malignancies such as pancreatic ductal adenocarcinoma, ROR2 is overexpressed in both tumor cells and the stromal microenvironment, correlating with poor clinical outcomes (28-30). In osteoarthritis, blockade of ROR2 attenuates joint degradation (31), and in cardiovascular disease, the WNT5A–ROR2 signaling axis regulates cholesterol metabolism and modulates inflammatory processes in atherosclerosis (32). Among the 19 human Wnt ligands, WNT1, WNT5A, and WNT7A have been shown to interact with ROR2 at the molecular level (14, 33-35). In IPF lung tissue, we observed co-localization of ROR2 with COL1A1 as well as with WNT1, WNT5A, and WNT7A, suggesting that ROR2 may mediate tissue remodeling, cell migration, and fibrotic progression via these ligands. Elevated WNT1 levels have been reported in BAL fluid from bleomycin-treated mice, indicating a conserved role in fibrotic lung injury (11), and functionally, WNT1 promotes myofibroblast differentiation and extracellular matrix production (36). WNT5A was detected in BAL fluid and fibrotic lung tissue and is expressed in epithelial, endothelial, and smooth muscle cells (12, 37-39). WNT7A, predominantly secreted by basal-like epithelial cells, functions through paracrine signaling to induce epithelial–mesenchymal transition, fibroblast-to-myofibroblast transition, and extracellular matrix production—key fibrogenic processes in IPF (13, 40). ROR2, acting as a receptor for WNT5A, activates non-canonical signaling pathways such as JNK and ROCK, which promote cytoskeletal remodeling and latent TGF-β activation (28, 41). These molecular events are critical for fibroblast activation and tissue fibrosis. In our cohort, elevated ROR2 levels were associated with increased mortality, whereas Wnt ligands alone were not independently significant. Nevertheless, their co-localization with ROR2 and documented roles in fibroblast activation suggest potential contributions to IPF pathogenesis, highlighting the ROR2–Wnt axis as a focus for further mechanistic studies. However, our study has limitations. First, BAL was obtained from the most affected lower lobe in IPF and the right middle lobe in controls, which may have affected biomarker levels despite standardized procedures. Secondly, the study included a small and younger control group, and due to the limited sample size and event count, multivariate and validation analyses were not feasible, increasing the risk of overfitting. Consequently, although DL_{CO} is a clinically important prognostic factor, it was not retained in the final multivariate Cox model. While penalized Cox methods such as ridge or LASSO could potentially improve model stability in small-sample settings, we opted for conventional backward selection to maintain interpretability of HR. Thirdly, multiple biomarker comparisons and treatment of values below the detection limit were not formally adjusted, which may have influenced statistical significance. Finally, given the observational nature and lack of external validation, the findings should be regarded as exploratory and hypothesis-generating. Further large-scale studies are warranted to confirm the diagnostic and prognostic value of ROR2 and Wnt signaling in IPF. In conclusion, ROR2 is independently associated with disease progression in IPF and represents a promising biomarker for identifying molecular endotypes and assessing clinical risk. Exploratory analysis suggests that interactions with WNT5A may define a subset of patients with distinct prognosis, although this requires further validation. Larger, externally validated studies are needed to confirm these findings, and mechanistic investigations are warranted to clarify the precise role of ROR2 within the WNT signaling network and its potential as a therapeutic target.

Acknowledgements: The biospecimens and data used for this study were provided by the Biobank of Soonchunhyang University Bucheon Hospital, a member of the Korea Biobank Network (KBN4_A06). We would like to thank Myung-Ran Lee, Young-Gil Lee, Jeong-Eun Lee, and Da-Jeong Jang for their assistance in the collection and distribution of biospecimens and their clinical information.

Funding: This research was supported by Basic Science Research Program through the National Research Foundation of Korea (NRF) funded by the Ministry of Education (RS-2023-00240858 and RS-2025-25419099).

Data Statement: The datasets used and/or analyzed during the current study available from the corresponding author on reasonable request.

Author Contributions: JUL, CSP, HSC: Conceptualization; JUL, SLP: Data curation; CSP, JUL: Funding acquisition; MSK, HGH, JHK, HSC: Methodology; JUL, SLP, MKK, ES: Validation; JUL, SLP: Visualization; JUL, SLP, CSP, HSC: Writing – original draft; all authors: Writing – review and editing.

Conflict of Interest Statement: Each author declares that he or she has no commercial associations (e.g. consultancies, stock ownership, equity interest, patent/licensing arrangement etc.) that might pose a conflict of interest in connection with the submitted article

Declaration on the Use of AI: During the preparation of this work the authors used Wordvice (Wordvice Inc., Des Moines, Iowa, USA) in order to enhance the language quality and readability. After using this tool, the authors reviewed and edited the content as needed and takes full responsibility for the content of the publication.

References

1. Richeldi L, Collard HR, Jones MG. Idiopathic pulmonary fibrosis. Lancet. 2017;389(10082):1941-52. Epub 20170330. doi: 10.1016/s0140-6736(17)30866-8. PubMed PMID: 28365056.
2. Sakai N, Tager AM. Fibrosis of two: Epithelial cell-fibroblast interactions in pulmonary fibrosis. Biochim Biophys Acta. 2013;1832(7):911-21. Epub 20130314. doi: 10.1016/j.bbadis.2013.03.001. PubMed PMID: 23499992; PubMed Central PMCID: PMC4041487.
3. Chambers RC, Mercer PF. Mechanisms of alveolar epithelial injury, repair, and fibrosis. Ann Am Thorac Soc. 2015;12 Suppl 1(Suppl 1):S16-20. doi: 10.1513/AnnalsATS.201410-448MG. PubMed PMID: 25830828; PubMed Central PMCID: PMC4430974.
4. Hinz B. Mechanical aspects of lung fibrosis: a spotlight on the myofibroblast. Proc Am Thorac Soc. 2012;9(3):137-47. doi: 10.1513/pats.201202-017AW. PubMed PMID: 22802288.
5. Wynn TA. Integrating mechanisms of pulmonary fibrosis. J Exp Med. 2011;208(7):1339-50. doi: 10.1084/jem.20110551. PubMed PMID: 21727191; PubMed Central PMCID: PMC3136685.
6. Kulkarni T, O'Reilly P, Antony VB, Gaggar A, Thannickal VJ. Matrix Remodeling in Pulmonary Fibrosis and Emphysema. Am J Respir Cell Mol Biol. 2016;54(6):751-60. doi: 10.1165/rcmb.2015-0166PS. PubMed PMID: 26741177; PubMed Central PMCID: PMC4942216.
7. Logan CY, Nusse R. The Wnt signaling pathway in development and disease. Annu Rev Cell Dev Biol. 2004;20:781-810. doi: 10.1146/annurev.cellbio.20.010403.113126. PubMed PMID: 15473860.
8. Komiya Y, Habas R. Wnt signal transduction pathways. Organogenesis. 2008;4(2):68-75. doi: 10.4161/org.4.2.5851. PubMed PMID: 19279717; PubMed Central PMCID: PMC2634250.
9. Chilosi M, Poletti V, Zamò A, et al. Aberrant Wnt/beta-catenin pathway activation in idiopathic pulmonary fibrosis. Am J Pathol. 2003;162(5):1495-502. doi: 10.1016/s0002-9440(10)64282-4. PubMed PMID: 12707032; PubMed Central PMCID: PMC1851206.
10. Shi J, Li F, Luo M, Wei J, Liu X. Distinct Roles of Wnt/β-Catenin Signaling in the Pathogenesis of Chronic Obstructive Pulmonary Disease and Idiopathic Pulmonary Fibrosis. Mediators Inflamm. 2017;2017:3520581. Epub 20170509. doi: 10.1155/2017/3520581. PubMed PMID: 28588349; PubMed Central PMCID: PMC5447271.
11. Königshoff M, Kramer M, Balsara N, et al. WNT1-inducible signaling protein-1 mediates pulmonary fibrosis in mice and is upregulated in humans with idiopathic pulmonary fibrosis. J Clin Invest. 2009;119(4):772-87. Epub 20090316. doi: 10.1172/jci33950. PubMed PMID: 19287097; PubMed Central PMCID: PMC2662540.
12. Vuga LJ, Ben-Yehudah A, Kovkarova-Naumovski E, et al. WNT5A is a regulator of fibroblast proliferation and resistance to apoptosis. Am J Respir Cell Mol Biol. 2009;41(5):583-9. Epub 20090227. doi: 10.1165/rcmb.2008-0201OC. PubMed PMID: 19251946; PubMed Central PMCID: PMC2778165.
13. Huang G, Liang J, Huang K, et al. Basal Cell-derived WNT7A Promotes Fibrogenesis at the Fibrotic Niche in Idiopathic Pulmonary Fibrosis. Am J Respir Cell Mol Biol. 2023;68(3):302-13. doi: 10.1165/rcmb.2022-0074OC. PubMed PMID: 36318668; PubMed Central PMCID: PMC9989475.

14. Winkel A, Stricker S, Tylzanowski P, et al. Wnt-ligand-dependent interaction of TAK1 (TGF-beta-activated kinase-1) with the receptor tyrosine kinase Ror2 modulates canonical Wnt-signalling. Cell Signal. 2008;20(11): 2134-44. Epub 20080816. doi: 10.1016/j.cellsig.2008.08 .009. PubMed PMID: 18762249.
15. Lee JU, Cheong HS, Shim EY, et al. Gene profile of fibroblasts identify relation of CCL8 with idiopathic pulmonary fibrosis. Respir Res. 2017;18(1):3. Epub 20170105. doi: 10.1186/s12931-016-0493-6. PubMed PMID: 28057004; PubMed Central PMCID: PMC5216573.
16. Son JH, Lee JU, Chin S, et al. Upregulation of receptor tyrosine kinase-like orphan receptor 2 in idiopathic pulmonary fibrosis. Korean J Intern Med. 2021;36(4):914-23. Epub 20200921. doi: 10.3904/kjim.2019.270. PubMed PMID: 32951408; PubMed Central PMCID: PMC8273837.
17. Raghu G, Collard HR, Egan JJ, et al. An official ATS/ERS/JRS/ALAT statement: idiopathic pulmonary fibrosis: evidence-based guidelines for diagnosis and management. Am J Respir Crit Care Med. 2011;183(6):788-824. doi: 10.1164/rccm.2009-040GL. PubMed PMID: 21471066; PubMed Central PMCID: PMC5450933.
18. Raghu G, Remy-Jardin M, Myers JL, et al. Diagnosis of Idiopathic Pulmonary Fibrosis. An Official ATS/ERS/JRS/ALAT Clinical Practice Guideline. Am J Respir Crit Care Med. 2018;198(5):e44-e68. doi: 10.1164/rccm.201807 -1255ST. PubMed PMID: 30168753.
19. Park CS, Chung SW, Ki SY, et al. Increased levels of interleukin-6 are associated with lymphocytosis in bronchoalveolar lavage fluids of idiopathic nonspecific interstitial pneumonia. Am J Respir Crit Care Med. 2000;162(3 Pt 1): 1162-8. doi: 10.1164/ajrccm.162.3.9906007. PubMed PMID: 10988147.
20. Meyer KC, Raghu G, Baughman RP, et al. An official American Thoracic Society clinical practice guideline: the clinical utility of bronchoalveolar lavage cellular analysis in interstitial lung disease. Am J Respir Crit Care Med. 2012;185(9):1004-14. doi: 10.1164/rccm.201202-0320ST. PubMed PMID: 22550210.
21. Meyer KC. Bronchoalveolar lavage as a diagnostic tool. Semin Respir Crit Care Med. 2007;28(5):546-60. doi: 10.1055/s-2007-991527. PubMed PMID: 17975782.
22. Shakhov AS, Kovaleva PA, Churkina AS, Kireev, II, Alieva IB. Colocalization Analysis of Cytoplasmic Actin Isoforms Distribution in Endothelial Cells. Biomedicines. 2022;10(12). Epub 20221209. doi: 10.3390/biomedicines 10123194. PubMed PMID: 36551950; PubMed Central PMCID: PMC9775052.
23. DeLong ER, DeLong DM, Clarke-Pearson DL. Comparing the areas under two or more correlated receiver operating characteristic curves: a nonparametric approach. Biometrics. 1988;44(3):837-45. PubMed PMID: 3203132.
24. Mikels AJ, Nusse R. Purified Wnt5a protein activates or inhibits beta-catenin-TCF signaling depending on receptor context. PLoS Biol. 2006;4(4):e115. Epub 20060404. doi: 10.1371/journal.pbio.0040115. PubMed PMID: 16602827; PubMed Central PMCID: PMC1420652.
25. Wang K, Ma F, Arai S, et al. WNT5a Signaling through ROR2 Activates the Hippo Pathway to Suppress YAP1 Activity and Tumor Growth. Cancer Res. 2023;83(7): 1016-30. doi: 10.1158/0008-5472.Can-22-3003. PubMed PMID: 36622276; PubMed Central PMCID: PMC10073315.
26. Zhou Y, Kipps TJ, Zhang S. Wnt5a Signaling in Normal and Cancer Stem Cells. Stem Cells Int. 2017;2017:5295286. Epub 20170412. doi: 10.1155/2017/5295286. PubMed PMID: 28491097; PubMed Central PMCID: PMC5405594.
27. Zhou Y, Ling T, Shi W. Current state of signaling pathways associated with the pathogenesis of idiopathic pulmonary fibrosis. Respir Res. 2024;25(1):245. Epub 20240617. doi: 10.1186/s12931-024-02878-z. PubMed PMID: 38886743; PubMed Central PMCID: PMC11184855.
28. Menck K, Heinrichs S, Baden C, Bleckmann A. The WNT/ROR Pathway in Cancer: From Signaling to Therapeutic Intervention. Cells. 2021;10(1). Epub 20210112. doi: 10.3390/cells10010142. PubMed PMID: 33445713; PubMed Central PMCID: PMC7828172.
29. Debebe Z, Rathmell WK. Ror2 as a therapeutic target in cancer. Pharmacol Ther. 2015;150:143-8. Epub 20150119. doi: 10.1016/j.pharmthera.2015.01.010. PubMed PMID: 25614331; PubMed Central PMCID: PMC9236825.
30. Huang J, Fan X, Wang X, et al. High ROR2 expression in tumor cells and stroma is correlated with poor prognosis in pancreatic ductal adenocarcinoma. Sci Rep. 2015;5:12991. Epub 20150811. doi: 10.1038/srep12991. PubMed PMID: 26259918; PubMed Central PMCID: PMC4531333.
31. Thorup AS, Strachan D, Caxaria S, et al. ROR2 blockade as a therapy for osteoarthritis. Sci Transl Med. 2020;12(561). doi: 10.1126/scitranslmed.aax3063. PubMed PMID: 32938794.
32. Zhang CJ, Zhu N, Liu Z, et al. Wnt5a/Ror2 pathway contributes to the regulation of cholesterol homeostasis and inflammatory response in atherosclerosis. Biochim Biophys Acta Mol Cell Biol Lipids. 2020;1865(2):158547. Epub 20191031. doi: 10.1016/j.bbalip.2019.158547. PubMed PMID: 31678514.
33. Billiard J, Way DS, Seestaller-Wehr LM, Moran RA, Mangine A, Bodine PV. The orphan receptor tyrosine kinase Ror2 modulates canonical Wnt signaling in osteoblastic cells. Mol Endocrinol. 2005;19(1):90-101. Epub 20040923. doi: 10.1210/me.2004-0153. PubMed PMID: 15388793.
34. Mikels A, Minami Y, Nusse R. Ror2 receptor requires tyrosine kinase activity to mediate Wnt5A signaling. J Biol Chem. 2009;284(44):30167-76. Epub 20090831. doi: 10.1074/jbc.M109.041715. PubMed PMID: 19720827; PubMed Central PMCID: PMC2781572.
35. Chakraborty A, Nathan A, Orcholski M, et al. Wnt7a deficit is associated with dysfunctional angiogenesis in pulmonary arterial hypertension. Eur Respir J. 2023;61(6). Epub 20230608. doi: 10.1183/13993003.01625-2022. PubMed PMID: 37024132; PubMed Central PMCID: PMC10259331.

36. Song P, Zheng JX, Liu JZ, et al. Effect of the Wnt1/β-catenin signalling pathway on human embryonic pulmonary fibroblasts. Mol Med Rep. 2014;10(2):1030-6. Epub 20140521. doi: 10.3892/mmr.2014.2261. PubMed PMID: 24859686.
37. Kumawat K, Gosens R. WNT-5A: signaling and functions in health and disease. Cell Mol Life Sci. 2016;73(3):567-87. Epub 20151029. doi: 10.1007/s00018-015-2076-y. PubMed PMID: 26514730; PubMed Central PMCID: PMC4713724.
38. Liu T, Gonzalez De Los Santos F, Hirsch M, Wu Z, Phan SH. Noncanonical Wnt Signaling Promotes Myofibroblast Differentiation in Pulmonary Fibrosis. Am J Respir Cell Mol Biol. 2021;65(5):489-99. doi: 10.1165/rcmb.2020-0499OC. PubMed PMID: 34107237; PubMed Central PMCID: PMC8641847.
39. Newman DR, Sills WS, Hanrahan K, et al. Expression of WNT5A in Idiopathic Pulmonary Fibrosis and Its Control by TGF-β and WNT7B in Human Lung Fibroblasts. J Histochem Cytochem. 2016;64(2):99-111. Epub 20151104. doi: 10.1369/0022155415617988. PubMed PMID: 26538547; PubMed Central PMCID: PMC4812680.
40. Königshoff M, Eickelberg O. Listen to the WNT; It Talks: WNT7A Drives Epithelial-Mesenchymal Cross-Talk within the Fibrotic Niche in Idiopathic Pulmonary Fibrosis. Am J Respir Cell Mol Biol. 2023;68(3):239-40. doi: 10.1165/rcmb.2022-0479ED. PubMed PMID: 36525670; PubMed Central PMCID: PMC9989476.
41. Nishita M, Enomoto M, Yamagata K, Minami Y. Cell/tissue-tropic functions of Wnt5a signaling in normal and cancer cells. Trends Cell Biol. 2010;20(6):346-54. Epub 20100330. doi: 10.1016/j.tcb.2010.03.001. PubMed PMID: 20359892.

Annex

Table S1. Detection frequencies of ROR2 and Wnt ligands in BAL fluid from IPF patients and controls.

	IPF + (n, %)	IPF – (n, %)	Control + (n, %)	Control – (n, %)	χ^2 p-value
ROR2	109 (87.9%)	15 (12.1%)	1 (5.9%)	16 (94.1%)	< 0.001
WNT1	100 (80.6%)	24 (19.4%)	15 (88.2%)	2 (11.8%)	0.449
WNT5A	89 (71.8%)	35 (28.2%)	9 (52.9%)	8 (47.1%)	0.113
WNT7A	82 (66.1%)	42 (33.9%)	8 (47.1%)	9 (52.9%)	0.124

Data are presented as number and percentage of patients showing detectable "+" and undetectable "–" levels within each group. "+" indicates levels above the assay's detection limit. Statistical comparisons between groups were performed using the chi-square test. A p-value of less than 0.05 was considered statistically significant.